Available online at www.sciencedirect.com
ScienceDirect
International Journal of Coal Geology 71 (2007) 455–461
International Journal of COAL GEOLOGY
www.elsevier.com/locate/ijcoalgeo

Physical properties of shungite

Barbara Kwiecinska [a,*], Slawomira Pusz [b], Marta Krzesinska [b], Barbara Pilawa [b]

[a] *Faculty of Geology, Geophysics and Environment Protection, University of Science and Technology-AGH, Al. Mickiewicza 30, 30-059 Kraków, Poland*
[b] *Institute of Coal Chemistry, Polish Academy of Science, ul. Sowinskiego 5, 44-121 Gliwice, Poland*

Received 10 January 2006; received in revised form 11 April 2006; accepted 25 May 2006
Available online 3 November 2006

Abstract

This paper presents the results of physical parameters such as bulk porosity, true density, optical reflectance, dynamic elastic moduli, X-ray diffractograms and EPR spectra, determined for shungite. All shungite samples studied are considerably denser materials than anthracite — high rank coal with similar carbon content. Bright shungites were porous with the very dense matrix, while the dull shungite is compact, almost non-porous material. Elastic moduli of the dull shungite are generally higher than those of bright shungites and anthracite. All shungites studied (including anthracite) exhibit the directional dependence of elasticity. The maximum reflectance values of bright shungites are higher than those for dull shungite and anthracite. That corresponds with the denser matrix of these samples and suggests the greatest ordering of graphene layers in the case of bright shungites and also suggests some similarity to meta-anthracite from Paleozoic basins. Reflectance anisotropy of shungites studied are generally lower than that of anthracite. Ordering of graphene layers in bright shungite, as a high rank coal variety, is obvious, but lower anisotropy than that of anthracite is a surprise. X-ray studies confirm a high density of bright shungite. Interplanar distances d_{hkl} of the shungite (d_{002}=3.48 Å) are closer to those of anthracite (d_{002}=3.52 Å) than to those of graphite (d_{002}=3.35 Å). All results described here show the differences in molecular structure and degree of graphitisation of carbonaceous matter in bright, semi-bright and dull varieties of shungite. Our data could play a key role in production of materials composed of carbon nanoparticles.
© 2006 Published by Elsevier B.V.

Keywords: Shungite; True density; Dynamic elastic modulus; EPR spectrum; Optical reflectance; X-ray measurements

1. Introduction

Shungite represents highly condensed carbonaceous matter occurring in Precambrian metamorphosed sediments in Karelia, near Shunga village in the Trans-Onega area in Russia. The shungite holotype was examined and described by Inostrantsev (1879). Since that time many publications about shungite have appeared concerning different aspects of its geological and petrological features, genesis, structure and chemical composition (Bo3dyriew and Kowalew, 1937; Kumpan, 1949; Kwieciñska, 1968; Khavari-Khorasani and Murchison, 1979; Volkova and Bogdanova, 1983, 1986; Buseck and Huang, 1985; Jehlicka and Rouzaud, 1993; Mastalerz et al., 2000; Kovalevski et al., 2001). The published results exhibit considerable differences with respect to the origin and properties of organic matter accumulated in shungite or to its structural (crystalline) organization.

The samples of shungite examined in our studies were kindly provided by Dr. I. Volkova from the Geological Research Institute in St. Petersburg. In these samples we

* Corresponding author.
E-mail address: kwiecin@uci.agh.edu.pl (B. Kwiecinska).

0166-5162/$ - see front matter © 2006 Published by Elsevier B.V.
doi:10.1016/j.coal.2006.05.008

identified three varieties: bright, semi-bright and dull. All varieties are very hard and compact and show a conchoidal fracture. The bright variety is of steel-black colour with metallic lustre, while the dull variety has a numerous accumulations of inorganic substances (pyrite, quartz, clays, carbonates). Semi-bright variety has intermediate features. Microscopic observations under reflected light of all varieties did not show major differences, except that bright samples (1–3) were more homogeneous with a slight anisotropy visible under crossed nicols.

The goal of this paper is to contribute to a better understanding of some of the physical properties of shungite.

2. Experimental

2.1. Preparation of samples

Samples were prepared in pieces with frontal planes for the ultrasonic studies and as powder or granular samples for the EPR and optical studies as well as for the X-ray investigations.

2.2. Porosity

Both apparent and true densities were measured to determine the bulk porosity of the samples. Apparent density was determined by means of a balance with equipment for apparent density measurements for crumple samples or of irregular shape (type 770–910 KERN). The true density was measured using a helium gas displacement pycnometer type 1305 Micromeritics®. The porosity of shungites was calculated using an expression:

$$P(\%) = 100 \times [(\rho_{\text{true}} - \rho_{\text{app}})/(\rho_{\text{true}})] \quad (1)$$

where P is the porosity, ρ_{true} and ρ_{app} are the true and the apparent densities of a sample, respectively.

2.3. Ultrasonic velocity and dynamic elastic modulus

For the ultrasonic frequencies used, coal samples may be treated as homogeneous materials and the following equation can be applied for the determination of dynamic elastic moduli [Eq. (1)]:

$$E = \rho v^2 \quad (2)$$

where E — the dynamic elastic modulus, v — the velocity, with which a stress wave is propagated through a homogeneous material, and ρ — the density of the material. In the case of porous materials, it is necessary to distinguish bulk elasticity of material from its matrix (stiff backbone) elasticity. It is clear that, for the determination of bulk dynamic modulus by means of Eq. (2) an apparent density has to be chosen, i.e., $\rho = \rho_{\text{app}}$.

The dynamic elastic moduli were determined using ultrasonic velocity measurements. The velocity of longitudinal ultrasonic wave of frequency of 100 kHz was measured along every of three basic axes of monolithic sample using an ultrasonic tester (Tester CT1, UNIPAN-ULTRASONIC, Poland). Dynamic elastic moduli were determined from an apparent density and ultrasonic velocity using Eq. (2). Elastic anisotropy was calculated from a relation $E_{\max}/E_{\min}$, where $E_{\max}$ is a maximal value of dynamic elastic modulus among moduli determined for three mutually perpendicular directions of a block sample. Similarly, $E_{\min}$ was defined as minimal value of elastic modulus. An isotropic structure is described by elastic anisotropy parameter equal to 1. Materials with $E_{\max}/E_{\min} > 1$ are elastically anisotropic. The higher the value of $E_{\max}/E_{\min}$, the larger the elastic anisotropy. Directions in a sample characterized by maximal, mid and minimal values of elastic modulus were denoted by letters a, b and c, respectively.

The dynamic elastic moduli of all samples studied (except of bright 1) were determined for block samples with three mutually perpendicular pairs of parallel frontal planes. In the case of the bright 1 shungite, moduli were measured along two mutually perpendicular directions for grains using a buffer rod.

2.4. Microscopic study

Reflectance measurements, as well as microscopic observations were made with reflected light optical microscope Axioskop MPM 200 (Opton-Zeiss, Germany). Reflectance measurements were made on randomly oriented shungite grains with a diameter (in mm) of $1.0 < z < 5.0$, using monochromatic linearly polarised light of $\lambda = 546$ nm, with immersion oil. Fifty to 200 points per sample were measured. $R'_{\max}$ and $R'_{\min}$ values were automatically recorded by means of a MSP 20 microprocessor during rotation of the microscopic stage through 360°. Additionally, for bright shungites reflectance measurements on natural cleavage surface (R_{nat}) were also carried out.

2.5. Electron paramagnetic resonance parameters

The studies of shungite samples by electron paramagnetic resonance (EPR) spectroscopy were performed using an X-band (9.3 GHz) EPR spectrometer

Table 1
Apparent (ρ_{app}) and true densities (ρ_{true}), porosity (P), ultrasonic velocities (v), elastic moduli (E), and elastic anisotropy (*) data quoted from Krzesińska et al., 2005)

Sample-variety	ρ_{app} (g/cm^3)	ρ_{true} (g/cm^3)	P (%)	Ultrasonic velocity			Elastic moduli			E_a/E_c
				v_a (m/s)	v_b (m/s)	v_c (m/s)	E_a (GPa)	E_b (GPa)	E_c (GPa)	
Dull	2.156	2.182	1.19	3268	2716	2313	23.029	15.906	11.536	2.00
Semi bright	1.939	2.250	13.82	2860	2745	2552	15.86	14.61	12.63	1.26
Bright 1	1.839	2.008	8.42	2682	2057	–	13.228	7.781	–	–
Bright 2	1.848	2.167	14.72	2678	2295	1688	13.253	9.733	5.266	2.52
Bright 3	1.848	1.958	5.62	3474	3058	2416	22.303	17.281	10.787	2.07
Anthracite*)	1.569	1.632	3.86	2825	2376	1787	12.623	8.907	5.137	2.85

(RADIOPAN, Poland) with magnetic modulation 100 kHz. The microwave frequency was recorded.

The EPR spectra of both organic paramagnetic centers and Fe^{3+} ions were collected by an IBM computer connected with spectrometer. The spectra were taken with high attenuation of microwave power 20 dB (about 0.7 mW) to avoid signal saturation. The parameters of the EPR spectra: amplitude A, linewidth ΔB_{pp} and g-factor, were evaluated. The g-factor was calculated from resonance condition [Eq. (3)]:

$$g = h\nu/\beta B_r \quad (3)$$

where: h — Planck constant, ν — microwave frequency, β — Bohr magnethon, and B_r — resonance magnetic field.

2.6. X-ray study

X-ray investigations were carried out on powdered samples using a Philips X-pert diffractometer with a graphite monochromator under the following conditions: Cu Kα radiation, scanning speed 0.02° (2θ) /1 s, the range recorded 3–71° (2θ), quartz as an internal standard.

3. Results and discussion

The physical parameters for shungite, obtained by EPR spectroscopy, optical microscopy, X-ray diffraction, densimetry and ultrasonic technique were compared with those obtained for Svierdlovsk anthracite (Ukraine) with carbon content C=94.9 wt.%. The data for anthracite were quoted from Krzesińska et al. (2005). The values of apparent (ρ_{app}) and true densities (ρ_{true}), ultrasonic velocities (v), elastic moduli (E), and elastic anisotropy are presented in Table 1, while optical reflectance, X-ray parameters and EPR parameters are shown in Tables 2, 3, and 4, respectively.

Fig. 1 shows the true and apparent densities (a) as well as the bulk porosity (b) calculated using Eq. (1). Anthracite belongs to the high rank coals with similar carbon content as shungite, but its both densities are considerably lower that those of shungite.

The bright varieties of shungite are the most porous materials among the samples studied. Although they are more porous materials than anthracite, their matrix is very dense, denser even than that of the anthracite. Dull shungite was found as compact, almost non-porous material.

Fig. 2 shows the dynamic elastic moduli determined for three mutually perpendicular directions. Elastic moduli of dull shungite are distinctly higher than those of bright shungite (except of the bright 3) and anthracite; that is clear, because dull shungite is almost non-porous material (P=1.19%) with high apparent density. Shungite bright 3 is the least porous of all bright varieties that

Table 2
Optical parameters R (%) and carbon content C^{daf} (wt.%)

Sample-variety	R_{random} %	R_{max} %	R_{min} %	R_m %	Bireflectance ($R_{max}-R_{min}$)	$R_{nat/random}$ %	C^{daf} [wt.%]
Dull	4.87	5.94	3.59	4.61	2.35	–	89.9
Semi-bright	8.44	10.58	4.14	6.62	6.44	–	92.1
Bright 1	6.32	7.15	5.17	6.08	1.98	9.83	96.9–
Bright 2	6.17	7.01	4.85	5.83	2.16	11.40	96.2
Bright 3	6.12	7.66	5.40	6.43	2.26	11.04	93.7
Anthracite	–	6.27	3.9	4.94	2.37	–	94.9

Note: R_{random} — measured mean reflectance value, R_{max} — measured mean maximum reflectance value, R_{min} — measured mean minimum reflectance value, R_m — calculated mean reflectance value, ($\sqrt{}$ R_{max}*R_{min}), $R_{nat/random}$ — mean reflectance value measured on natural cleavage surface.

Table 3
X-ray parameters of graphite, shungite and anthracite

d_{hkl}	Graphite	Shungite B1	Anthracite
(002)	3.35	3.48	3.52
(100)	2.09	2.10	2.10
(004)	1.67	–	–
(110)	1.23	1.228 [a]	1.195 [a]

[a] Weakly visible reflex.

explains a high ultrasonic velocity and consequently, a high dynamic elastic modulus.

The maximal values of R_{max} of bright shungite are higher than those for dull shungite and anthracite (Table 2). That correlates with the rank of samples studied and suggests the greatest ordering of graphene layers in the case of bright shungite, meaning the highest degree of structural order. It also corresponds with the denser matrix (true density) of these samples. It is worth noting that the reflectance measured on natural cleavage surfaces is higher in case of bright varieties and reaches values above 9%.

X-ray studies have confirmed a high density of bright shungite. Interplanar distances d_{hkl} of shungite (d_{002}=3.48 Å) are closer to those of anthracite (d_{002}=3.52 Å) than to those of graphite (d_{002}=3.35 Å) (Table 3, Fig. 3). It means that the degree of carbon crystallinity in shungite is rather low according to Buseck and Huang (1985), Volkova and Bogdanova (1986), Kwieciñska and Petersen (2004).

Fig. 4 shows the elastic and optical anisotropy of the samples studied. The elastic anisotropy of bright shungite is higher than that of dull and semi-bright varieties, but lower than that of anthracite. The semi-bright shungite was found as almost isotropic material, while all remaining samples including anthracite exhibit elastically anisotropic structure with parameter $E_{max}/E_{min}>2$.

The optical anisotropy of shungites studied is generally lower than that of anthracite. The semi-bright shungite is an exception. It has a mosaic, coke-like microscopic structure, different from the other shungites and its optical anisotropy is extremely high. Ordering of graphene layers in bright shungite, as highly aromatic

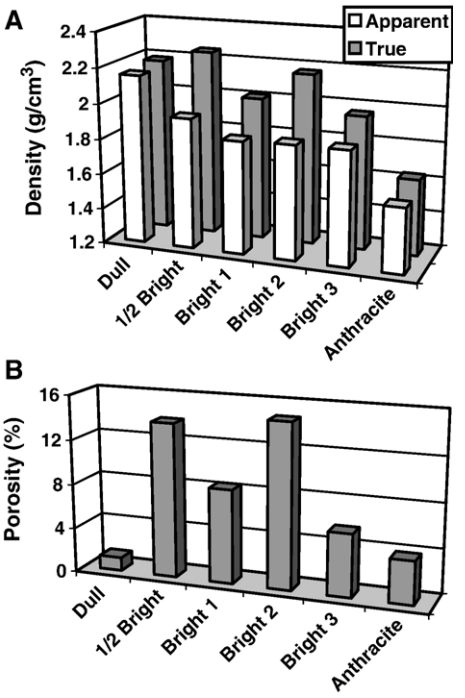

Fig. 1. True and apparent densities (A) and porosity (B) of the samples studied. (1/2 bright=semi-bright).

organic material, is obvious, but lower anisotropy than that of anthracite is a surprise.

Two lines at magnetic fields 334 mT (I EPR line) and 150 mT (II EPR line) were measured in the experimental EPR spectra of all samples studied. Fig. 5A shows the exemplary first line (I EPR line) of EPR spectra for bright and dull shungites, while Fig. 5B shows the second line (II EPR line). Organic paramagnetic centers and probably paramagnetic Fe^{3+} ions are responsible for the two EPR lines, respectively. EPR lines of organic paramagnetic centers were measured at 334 mT for all studied shungites. EPR lines of paramagnetic Fe^{3+} ions at 150 mT were measured only for dull and bright 1 shungites.

The following parameters of the recorded EPR lines: amplitudes A, g-factors and line widths ΔB_{pp} are presented

Table 4
Amplitudes A, g factors and linewidths ΔB_{pp} of both lines (I and II) in EPR spectra

Sample-variety	I EPR LINE			II EPR LINE		
	A [a.u.]	g (±0.0002)	ΔB_{pp} [±0.02 mT]	A [a.u.]	g (±0.0002)	ΔB_{pp} [±0.02 mT]
Dull	0.014	2.0033	2.54	0.002	4.6750	15.54
Semi-bright	8.981	2.0033	0.41	–	–	–
Bright 1	0.082	2.0029	1.00	0.001	4.2878	14.17
Bright 2	0.089	2.0027	2.06	–	–	–
Bright 3	0.886	2.0028	1.28	–	–	–
Anthracite	10.00	2.0029	0.1	–	–	–

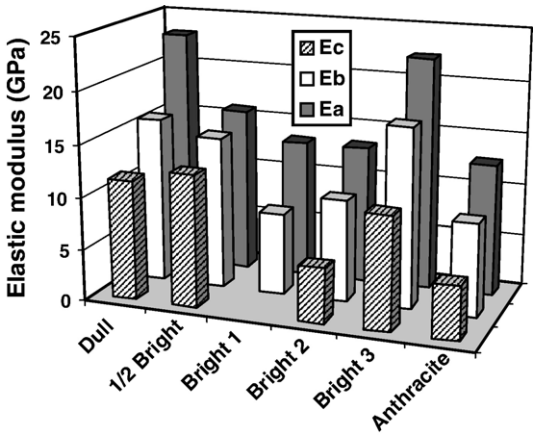

Fig. 2. Dynamic elastic modulus of the samples studied. (1/2 bright= semi-bright).

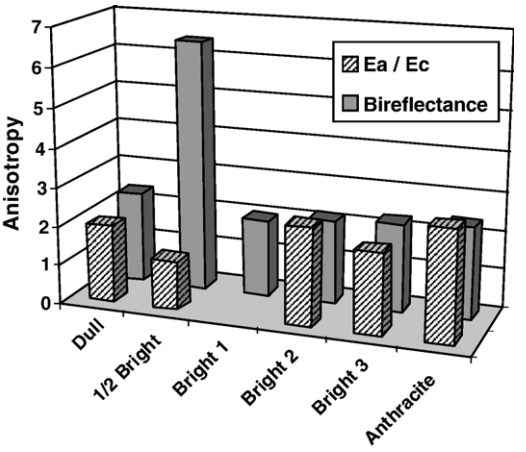

Fig. 4. Elastic and optical anisotropy of the samples studied. (1/2 bright= semi-bright).

in Table 4. Amplitude of the I EPR lines resulted from organic paramagnetic centers of bright shungites was considerably higher than that of dull shungite. π-electrons delocalized on the large multi-ring aromatic units with g-factor 2.0029 mainly exist in bright shungites. Properties of paramagnetic centers in semi-bright shungite and anthracite are similar. High amount of unpaired electrons characterizes these samples. The linewidths of EPR (I) lines of semi-bright shungite and anthracite indicate exchange interactions of unpaired magnetic moments in the samples. The relatively higher linewidth of EPR line of semi-bright shungite results from the additional dipolar interactions in its molecular units (Wertz and Bolton, 1986; Pilawa et al., 1995).

The electron paramagnetic resonance studies show that both dull and bright shungites reveal paramagnetism of organic substance. EPR analysis of dull and bright shungites points out that their organic matter differs in structure and molecular units. The highest linewidth (B_{pp}=2.54 mT) of EPR spectrum of dull shungite indicates strong dipolar interactions characteristic for units consisting from a few aromatic rings. Linewidths of the I EPR signals of bright shungite (B_{pp}=1.00–2.06 mT) indicate that larger aromatic units exist in these samples. The higher condensed aromatic units exist in the semi-bright variety with the lower EPR line width at 0.41 mT.

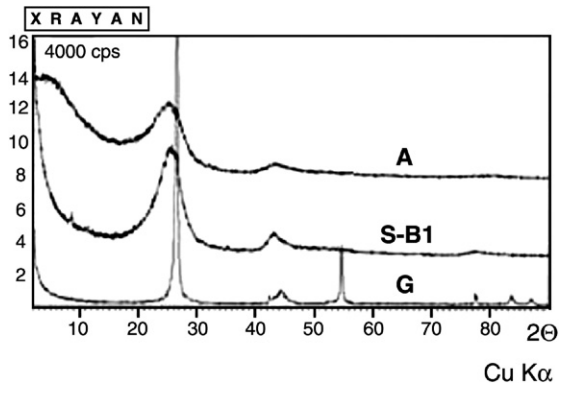

Fig. 3. X-ray diffractograms of graphite (G), representative shungite (S) and anthracite (A).

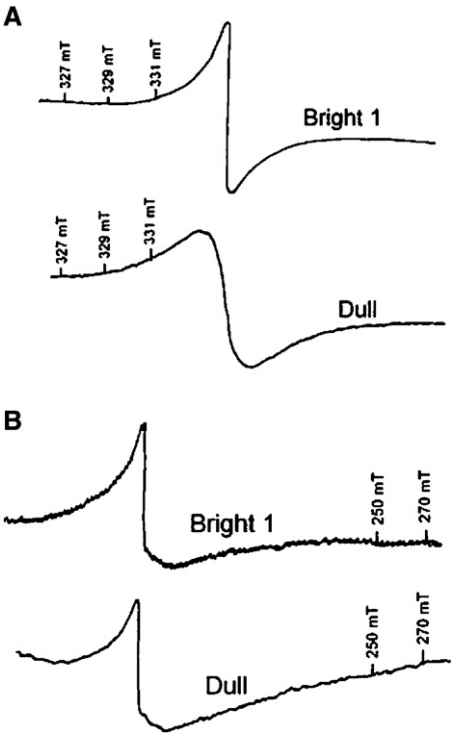

Fig. 5. The EPR spectra for the first EPR line - I (A) and for the second EPR line - II (B) for shungites.

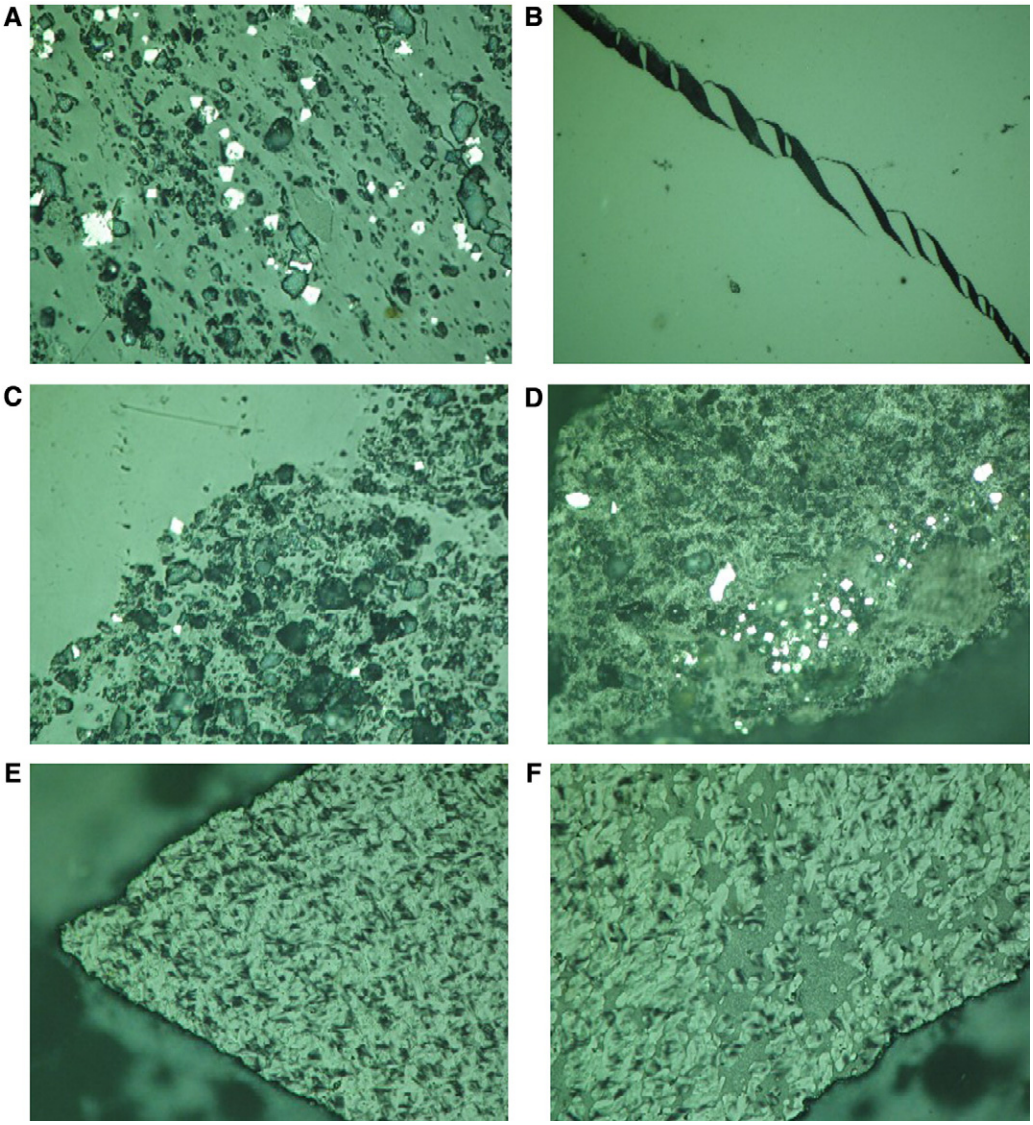

Fig. 6. Optical microscopy images (magnification 500×, immersion oil), (A) — bright shungite with pyrite grains (bright 1), (B) — bright shungite with specific cracks (bright 3), (C) — porous and non-porous areas in bright shungite (bright 2), (D) — dull shungite, (E) — semi-bright shungite – coke-like mosaic structure, (F) — porosity of semi-bright shungite.

The second EPR line interpreted as resulted from paramagnetic centers of iron coupled with pyrite is present in both shungites (dull and bright 1). The lower amplitude of the II EPR line with g value 4.2878 was observed for bright variety.

In the case of the dull shungite, the first EPR line describes paramagnetic centers of aromatic units, as well as of iron coupled with carbonates.

Fig. 6 presents optical microscopy images of the samples studied. Microscopic observations have shown that bright shungites are almost pure, highly homogeneous organic substance (Fig. 6A) containing small amounts of pyrite (small grains) (Fig. 6B). In places, close to homogeneous, compact areas of bright shungites, there are strongly porous zones where irregularly shaped pores are fulfilled by inorganic matter (Fig. 6C). Dull shungite is a rather high ash type which contains a lot of minerals embedded in organic matrix (Fig. 6D).

3.1. Properties of the semi-bright shungite

The semi-bright shungite has extreme properties that are different to those of high rank coals, that is

anthracite. Among the shungite samples it is characterized by:

- the highest true density equal to the density of graphite crystal,
- the high bulk porosity in comparison with the other samples,
- the highest optical reflectance R_{max},
- the highest optical anisotropy (bireflectance),
- the presence of a mosaic structure at the scale visible using the optical microscope,
- the lowest elastic anisotropy, resulting in a structure that is close to isotropic in terms of physical properties, and
- the highest number of spins expressed by the highest amplitude of the narrow EPR line.

The above properties can characterize material composed of ordered graphene units of small diameter consisting with several layers (Fig. 6E,F).

4. Conclusions

The results obtained in our study show the differences in molecular structure of organic matter in a range of varieties of shungite. The degree of graphitisation of carbon in shungite is rather low what as was already proved by several authors (Khavari-Khorasani and Murchison, 1979; Buseck and Huang, 1985; Volkova and Bogdanova, 1986; Jehlicka and Rouzaud, 1993). It seems that optical properties of bright shungites are similar to those of meta-anthracite of Paleozoic basins, but elastic features (ultrasonic velocity, EPR parameters) show the differences in internal structure of all types of shungite and anthracite. Following the data given by Rozhkova (2003) we can suggest that physical properties of shungite described in this paper could be used in comparative studies of materials composed of carbon nanodimensional particles and fullerenes.

Acknowledgements

The authors wish to thank Dr. I. Volkova from the Russian Geological Research Institute, St. Petersburg, for providing the samples of shungite and Mr. A. Gawel from the University of Science and Technology in Krakow for assistance with the X-ray analysis. The work carried out by B. Kwieciñska was partially supported by the AGH University of Science and Technology (Research project no.11.11.140.047).

References

Boldyriew, A.K., Kowalew, G.A., 1937. Rentgenometriczeskoje isledowanije szungita, antracita I kamiennogo ugla. Zap. Leningr. Inst., X, wyp. 2.

Buseck, P.R., Huang, B.J., 1985. Conversion of carbonaceous material to graphite during metamorphism. Geochim. Cosmochim. Acta 49, 2003–2016.

Inostrantsev, A.A., 1879. New end member of amorphous carbon. Gorn. Z. 2, 314–342 (in Russian).

Jehlicka, J., Rouzaud, J.N., 1993. Transmission electron microscopy of carbonaceous matter in Precambrian shungite from Karelia. In: Parnall, J., Kucha, H., Landais, R. (Eds.), Bitumens in Ore Deposits. Springer Verlag, Berin, pp. 53–60.

Khavari-Khorasani, G., Murchison, D., 1979. The nature of Karelian shungite. Chem. Geol. 26, 165–182.

Kovalevski, V.V., Buseck, P.R., Cowley, J.M., 2001. Comparison of carbon in shungite rocks to other natural carbons: an X-ray and TEM study. Carbon 39, 243–256.

Krzesiñska, M., Pusz, S., Koszorek, A., 2005. Elastic and optical anisotropy of the single-coal monolithic high-temperature (HT) carbonization products obtained on a laboratory scale. Energy Fuels 19, 1962–1970.

Kumpan, A.S., 1949. Sowriemennyje predstawlenija o wnutriennej strukturie uglej i zadaczi je dalnejszego uzuczenija. Zap. Wsesojuz. Min. Obszczestwa 3.

Kwiecińska, B., 1968. Investigation of shungite. Bull. Acad. Pol. Sci. Ser. Sci. Geol. Geogr. XVI/2, 61–65.

Kwiecińska, B., Petersen, H.I., 2004. Graphite, semi-graphite, natural coke, and natural char classification — ICCP system. Int. J. Coal Geol. 57, 99–116.

Mastalerz, M., Glikson, M., Stankiewicz, B.A., Volkova, I.B., Bustin, R.M., 2000. Organic and mineral matter in a Precambrian shungite deposit from Karelia, Russia. In: Glickson, M., Mastalerz, M. (Eds.), Organic Matter and Mineralisation. Kluwer Academic Publishers, London, pp. 102–119.

Pilawa, B., Wiêckowski, A.B., Trzebicka, B., 1995. Numerical analysis of EPR spectra of coal, macerals and extraction products, radiation. Phys. Chem. 45, 899–908.

Rozhkova, N.N., 2003. Shungite as a network of carbon nanoparticles. Process P231, 284.

Volkova, I.B., Bogdanova, M.V., 1983. O novich rastitelnuch structurach v shungitach Karelii. Dokl. Akad. Nauk SSSR 270 (2), 410–414 (in Russian).

Volkova, I., Bogdanova, M.V., 1986. Petrology and genesis of Karelian shungite-high rank coal. Int. J. Coal Geol. 6, 369–379.

Wertz, J.E., Bolton, J.R., 1986. Electron spin resonance. Elementary Theory and Practical Applications. Chapman and Hall, London, p. 136.